Original Article

Histological Evaluation of The Possible Therapeutic Effect of Pirfenidone on Bleomycin-Induced Pulmonary Fibrosis in Adult Male Albino Rats

Hend Shafik Bassiouny, Nagla Mohamed Salama, Alaa Serag El-dean Habib and Asmaa Mohamed Abdel-Hameed

Department of Histology, Faculty of Medicine, Cairo University, Egypt

ABSTRACT

Introduction and Aim of the Work: Idiopathic pulmonary fibrosis is a disease of unknown etiology that causes fibrosis in lung parenchyma with progressive irreversible nature with no appropriate therapy, so this study worked to evaluate the therapeutic effect of pirfenidone on a rat model of bleomycin-induced pulmonary fibrosis.

Materails and Methods: Thirty adult male albino rats were used in this study; classified into 5 groups: group I (control group), group II (prifenidone group), group III (model group), group IV (recovery group) and group V (treated group). Lung specimens were taken from rats of group IA and group III on the 14th day of the experiments while specimens from the rest of the groups were taken on the 28th day of the experiment. The specimens were subjected to biochemical analysis for malondialdehyde and glutathione as well as histological study using H & E, Masson's trichrome, toluidine blue stain for semithin sections and immunohistochemical stain for αSMA. The area percent of collagen and αSMA immunopositive cells were measured and statistically analysed using image analyser.

Results: Groups III and IV showed deposition of collagen in the thickened interalveolar septa and infiltration of interstitial tissue by inflammatory cells causing narrowing or even collapse of the intervening alveoli. There was a significant increase in the mean area percent of collagen and αSMA immunopositive cells with significant decrease in GSH and a significant increase in MDA as compared to control. Meanwhile group V showed restoring of normal lung architecture. There was a significant decrease in the mean area percent of collagen and αSMA immunopositive cells, significant increase in GSH and a significant decrease in MDA as compared to groups III and IV.

Conclusion: Pirfenidone was effective as antifibrotic agent with significant reduction of fibrosis and oxidative stress in rat model of lung fibrosis.

Received: 29 August 2021, **Accepted:** 16 September 2021

Key Words: Bleomycin, idiopathic pulmonary fibrosis, pirfenidone.

Corresponding Author: Asmaa M. Abdel Hameed, MD, Department of Histology, Faculty of Medicine, Cairo University, Egypt, **Tel.**: +20 10 9030 4335, **E-mail:** alabd.alsaleh@yahoo.com

ISSN: 1110-0559, Vol. 46, No.1

INTRODUCTION

Pulmonary fibrosis is the final outcome of various parenchymal lung disorders called interstitial lung disease (ILD). Idiopathic pulmonary fibrosis (IPF) is one of the most common subtypes of ILD, which is a chronic, progressive and generally fatal parenchymal lung disorder of unknown etiology with an approximate median survival of 2 to 5 years from diagnosis[1].

Although the triggering factor of IPF is still unknown, the pathogenesis of the disease is mostly caused by ineffective regeneration and wound repair of the lung epithelium. This leads to production of a series of cytokines and growth factors that in turn cause activation and proliferation of fibroblasts. Activated fibroblasts change into myofibroblasts, the hall mark of the disease, and secrete excessive amounts of extracellular matrix (ECM) that deposit in the tissue and cause loss of the normal architecture and integrity of the lung[2].

Different animal models were used to study IPF from different points of view among which is the bleomycin model. It is one of the oldest and most widely used models due its good reproducibility and ease of induction in addition to some histopathological criteria that resemble the human fibrotic process[3].

Bleomycin is a glycopeptide antibiotic used as a chemotherapeutic agent for lymphomas and testicular carcinomas[4]. The basis of bleomycin activity is generation of reactive oxygen species (ROS) that causes cytotoxicity and deoxyribonucleic acid (DNA) breakdown. This state is exaggerated in the lung due to its low content of bleomycin hydrolase; a bleomycin inactivating-enzyme. Thus, tissue injury resulting from bleomycin cause acute inflammation followed by subsequent chronic inflammation and fibrogenic state[5].

Despite striving, there was no appropriate therapy to reverse or stop the course of the disease. But with the discovery of antifibrotic agents, the therapeutic approach to IPF has been essentially changed[6].

 DOI: 10.21608/ejh.2021.93312.1554

Many researchers have studied the preventive potential of antifibrotic agents on bleomycin-induced fibrosis in prophylactic use, however, very few studies concernd with investigating the treatment of already established fibrosis[7].

Pirfenidone is an orally active small molecule with both antifibrotic and anti-inflammatory activities. Recent studies accredited its efficacy in a wide array of conditions as corneal alkali burn[8], tracheal stenosis[9], acute kidney injury[10] and cerebral ischemia[11].

Although the exact target of pirfenidone action is yet to be identified, its modulation of growth factors and cytokines with apparent reduction in underlying fibrosis ultimately guaranteed the usage of pirfenidone in treatment regimens of IPF[12].

Aim of this work is to evaluate the therapeutic effect of pirfenidone on bleomycin-induced pulmonary fibrosis in adult male albino rats, using biochemical, histological, immunohistochemical, and morphometric studies.

MATERIALS AND METHODS

Materials

Drugs

1. Bleomycin sulphate, Bleocel 15 IU, (CELON LABS Ltd. Telangana state,India) in the form of sterile lypholized vial. The solution for injection was prepared by adding 4.5 ml saline to the vial.
2. Pirfenidone, pirfenex, (CIPLA Ltd. Rorathang, India) in the form of 200mg tablets. The tablets were crushed and dissolved in 1 ml of 0.5% Carboxymethyl cellulose (CMC).

Animals

Thirty adult male albino rats of average body weight 200 grams and aged 10-12 weeks were purchased and raised in the Animal House of kasr Al-Ainy Hospital, Faculty of medicine, Cairo University. They were housed in a separate stainless-steel cages at room temperature, fed ad libitum with standardized chow and allowed free access to water. This study was conducted in accordance with ethical procedures and policies of the Animal Ethical Committee of Kasr Al-Ainy Faculty of medicine, Cairo University with approval number (cu III F 19 20).

Experimental design

The rats were divided into 5 groups:

Group I (Control group): It included 6 rats which were further subdivided into two subgroups:

- Subgroup IA (4 rats): Each rat received a single dose of 0.3ml saline through intratracheal (IT) instillation at day 0. Two of them were sacrificed at day 14 (control for model group) and the other two were sacrificed at day 28 (control for recovery group).
- Subgroup IB (2 rats): Each rat received a single dose of 0.3ml saline through IT instillation at day 0 and starting from day 14, they received orally 1 ml of 0.5% CMC once daily till they were sacrificed at day 28. Group II (pirfenidone group): It included 6 rats. Each rat received pirfenidone 100mg/kg body weight[13] dissolved in 1ml 0.5% CMC orally using intragastric tube, once daily starting at day 14 of the experiment till they were sacrificed at day 28.

Induction of pulmonary fibrosis model

The remaining eighteen rats are subjected to lung fibrosis by receiving single dose of bleomycin sulphate 5mg/kg dissolved in 0.3 ml saline for each rat through IT instillation at day 0 of the experiment[14]. Then they were classified as follow:

Group III (Model group): It included 6 rats on which pulmonary fibrosis were induced as described. All rats of this group were sacrificed at day 14 to assess for establishment of pulmonary fibrosis.

Group IV (Recovery group): It included 6 rats on which pulmonary fibrosis were induced as described. They were left without any further treatment and were sacrificed at day 28 to assess spontaneous recovery. Group V (Treated-group): It included 6 rats on which pulmonary fibrosis were induced as described. Starting from day 14 each rat received 100mg /kg body weight pirfenidone[13] dissolved in 1ml 0.5% CMC orally, once daily till they were sacrificed at day 28.

Methods

Induction of pulmonary fibrosis model

After overnight fasting, the rats were anesthetized (100mg/kg ketamine HCl and 10mg/kg xylazine) and a midline incision was made in the neck and the trachea was exposed by blunt dissection. Pulmonary fibrosis was induced by intratracheal administration of single dose 0.3ml of bleomycin (5mg/kg in saline). Injection was done by a 30 gauge needle under direct visualization into the trachea. The same procedure was performed for the control group with the exception that saline substituted for bleomycin[15].

Sample Collection and Processing

The animals belonging to experimental groups and corresponding control rats were sacrificed under general intraperitoneal anesthesia with sodium pentobarbital (100 mg/kg)[16] at the end of various durations previously mentioned. Lung specimens were obtained by performing a ventral midline incision, exposure, dissection and rapid excision to be subjected to the following:

A) Biochemical Study: Specimens from lower lobe of right lung were transferred in fresh state to the Biochemistry Department, Faculty of Medicine, Cairo University and the following was measured: 1. Glutathione (GSH) concentration: as a biomarker for intracellular antioxidant levels[17].

2. Malondialdehyde (MDA) concentration: as a biomarker for lipid peroxidation[18].

B) Histological Study: Specimens from the lower third of the left lung were fixed in 10% buffered formalin solution for 24 hours, dehydration in ascending grades of ethanol and embedded in paraffin. Serial sections of 7µm thickness were cut and subjected to the following:

1. Heamatoxylin and eosin (H.&E.) for general histological structure[19]
2. Masson's trichrome stain: to demonstrate collagen fibers[19]
3. Immunohistochemical staining for αSMA antibody[19]

For semithin sections, some specimens were fixed in 3% glutaraldehyde, postfixed in 1% osmium tetroxide, embedded in resin and cut at 1µm. The sections were stained with toluidine blue[20]

The sections for immunohistochemical stains were boiled for 10 min in 10 mM citrate buffer (AP9003) at pH 6 for antigen retrieval then incubated for 1h with the primary antibody. αSMA was the Primary antibody which is a mouse monoclonal antibody (Thermo Fischer scientific, CA, USA, catalogue number MS-113-R7) and It was supplied as 7.0ml of ready to use antibody (pre-diluted in 0.05mol/L Tris-HCL, PH 7.6 containing stabilizing protein and 0.015mol/L sodium azide). Ultravision detection system (TP-015-HD) was used to complete immunostaining and Mayer'shematoxylin (TA-060-MH) was used for counterstaining. Citrate buffer, Ultravision detection system and Mayer's hematoxylin were purchased from Labvision Thermo Scientific, Fremont, California, USA. Negative controls were done by applying same steps but omitting the step of adding the primary antibodies. Positive reaction in the specimen of human leiomyosarcoma appears as brown deposits in the cytoplasm of αSMA (positive) cells.

Morphometric study

- Ten non-overlapping randomly chosen fields (x400) from different sections of each rat of each group were investigated to measure:
- Area percent of collagen.
- The area percent of αSMA positive cells.

Measurements were taken using "Leica Qwin 500 C" image analyzer computer system Ltd. (Cambridge, England). (Histology Department, Faculty of Medicine, Cairo University).

Statistical Analysis

Quantitative data was summarized as means and standard deviation (SD) and compared using one-way analysis-of-variance (ANOVA). Any significant ANOVA was followed by post-hoc tukey test to detect which pairs of groups caused the significant difference[21]. *P values* <0.05 were considered statistically significant. Calculations were made on SPSS software version21.

RESULTS

No death occur in the control and pirfenidone groups (group I & II). on the other hand, one rat died in each of the model group, recovery group and treated group, and they were excluded from the study (17% mortality rate in each group). rats died one week after blomycin injection.

Histological results

All control subgroups showed similar histological results so, they were collectively named control group.

Hematoxylin and eosin stain: (Figures 1,2)

Examination of H&E stained sections of the lung of the control group exhibited normal lung parenchyma with preserved architecture of bronchioles, alveolar sacs, alveoli and interalveolar septa (Figures 1a,1b)

Group II demonstrated intact lung histological structure similar to that of control group with normal architecture of bronchioles, blood vessels, alveoli, alveolar sacs and interalveolar septa with normal pulmonary capillaries (Figure 1c,1d).

Group III revealed that ,in many regions, the interalveolar septa were thickened by inflammatory cells with narrowing or even collapse of the intervening alveoli (atelectasis). Other alveoli appeared enlarged (dilated). (Figures 2a,2b).

Group IV showed a progressive destruction of the lung architecture. Areas of narrowing and collapse of alveolar space were observed. Thickening of interalveolar septa and walls of the blood vessels was also noticed. Obvious cellular infiltration was detected in the interstitial tissue. Many alveolar spaces were flooded by numerous large foamy macrophages (Figures 2c,2d).

Meanwhile, sections from group V revealed that most of alveoli and interalveolar septa restored their normal architecture. However, few areas showed narrowing of some alveoli. Mild cellular infiltration of the interstitium was also observed (Figures 2e,2f).

Semithin, Toluidine blue stain: (Figure 3)

Control group showed normal alveoli with clear alveolar space. The alveoli were lined by type I pneumocytes, exhibiting flat nuclei, and type II pneumocytes which display round vesicular nuclei with prominent nucleolus and foamy cytoplasm. The interalveolar septa were thin containing blood capillaries (Figure 3a). Similarly the examination of semithin sections from group II revealed normal alveoli with thin interalveolar septa (Figure 3b).

Meanwhile, group III showed marked thickening of interalveolar septa with mononuclear cell infiltration. The inflammatory cells were mainly neutrophils, lymphocytes and macrophages (Figure 3c).

Group IV showed apparent thickening of interalveolar septa with evident mononuclear cell infiltration of both alveolar walls and alveolar spaces. Most alveoli were narrowed or collapsed and showed obvious appearance of type II pneumocytes. These cells frequently appeared larger than normal with increased cytoplasmic vacuoles (Figure 3d).

Group V showed many alveoli that restored their normal architecture with apparent thin interalveolar septa. However, few areas revealed thick interalveolar septa. Mild cellular infiltration was also observed (Figure 3e).

Masson's trichrome stain:(Figure 4)

Masson's trichrome stained sections of groups I and II revealed fine collagen fibers in the interalveolar septa, the adventitia of bronchioles and adventitia of the blood vessels (Figures 4a,4b).

Group III showed obvious deposition of collagen fibers in the thickened interalveolar septa as well as in the adventitia of bronchioles and blood vessels. (Figure 4c). Group IV revealed deposition of collagen fibers in the thickened interalveolar septa, adventitia of bronchioles and blood vessels (Figure 4d). meanwhile sections of group V revealed scattered fine collagen fibers in the interalveolar septa, adventitia of the bronchioles and that of the blood vessels (Figure 4e).

αSMA immunohistochemical stain: (Figure 5)

Sections of groups I and II showed positive cytoplasmic reaction in the smooth muscles investing bronchioles and blood vessels. Positive reaction at the knobs of the alveolar ducts was also detected (Figures 5a,5b).

Group III showed many cells with positive cytoplasmic reaction in the walls of alveoli and interalveolar septa. Positive reaction in the walls of blood vessels and bronchioles was also noticed (Figure 5c). Group IV showed numerous cells with positive immunoreactivity for αSMA in the interalveolar septa. Positive immunoreactivity in the walls of blood vessels and bronchioles was also noticed (Figure 5d).

Group V revealed few cells with cytoplasmic immunoreactivity for αSMA in the walls of alveoli and interalveolar septa. Positive immunoreactivity in the walls of blood vessels and bronchioles as well as knobs of alveolar ducts was also detected (Figure 5e).

Morphometric and statistical results (Table1, Histograms 1,2)

There was a significant increase in mean area percent of collagen in groups III, IV and V as compared with group I, while there was a non-significant increase as regard group II. Animals in group III showed non-significant increase as compared to group IV. Meanwhile, group V showed significant decrease in mean area percent of collagen as compared to groups III and IV respctively.

There was a significant increase in mean area percent of α SMA in groups III, IV and V as compared with group I, while there was a non-significant decrease as regard group II. Animals in group III showed a non-significant increase as compared to group IV. Meanwhile, group V showed a significant decrease in mean area percent of α SMA as compared to groups III and IV respctively.

Biochemical results: (Table 2, Histograms 3,4)

As compared with group I, there was a significant decrease in GSH concentration in groups III and IV, while there was a non-significant decrease as regard groups II and V. Animals in group III showed a non-significant increase in GSH concentration as compared to group IV. Meanwhile, group V showed a significant increase in GSH concentration as compared to groups III and IV respctively.

There was a significant increase in MDA concentration in groups III and IV as compared with group I, while there was a non-significant decrease as regard group II and a nonsignificant increase as regard group V. Animals in group III showed a non-significant decrease in MDA concentration as compared to group IV. Meanwhile, group V showed a significant decrease in MDA concentration as compared to groups III and IV respctively.

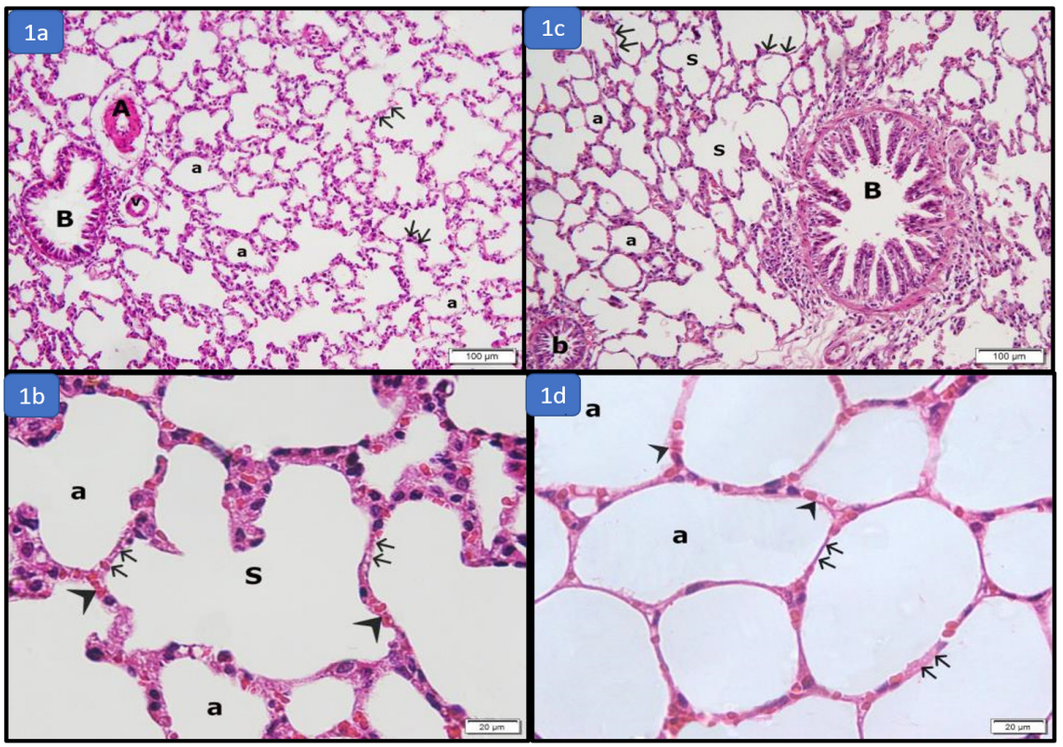

Fig. 1: Photomicrographs of sections in the lungs of rats stained with H&E (1a): control group showing normal bronchiole (B), many alvoeli (a) separated by thin interalveolar septa (arrows), arteriole (A) and venule (V). (x100). (1b): control group showing normal alveoli (a) with thin interalveolar septa (arrows) that contain blood capillaries (arrow heads). An alveolar sac is also seen (S). (x400). (1c): group II showing normal large (B) and small terminal (b) bronchioles, alveolar sacs (S), thin interalveolar septa (arrows) and alveoli (a). (x100). (1d): group II showing intact alveoli (a) with thin interalveolar septa (arrows) containing pulmonary capillaries (arrow heads). (x400).

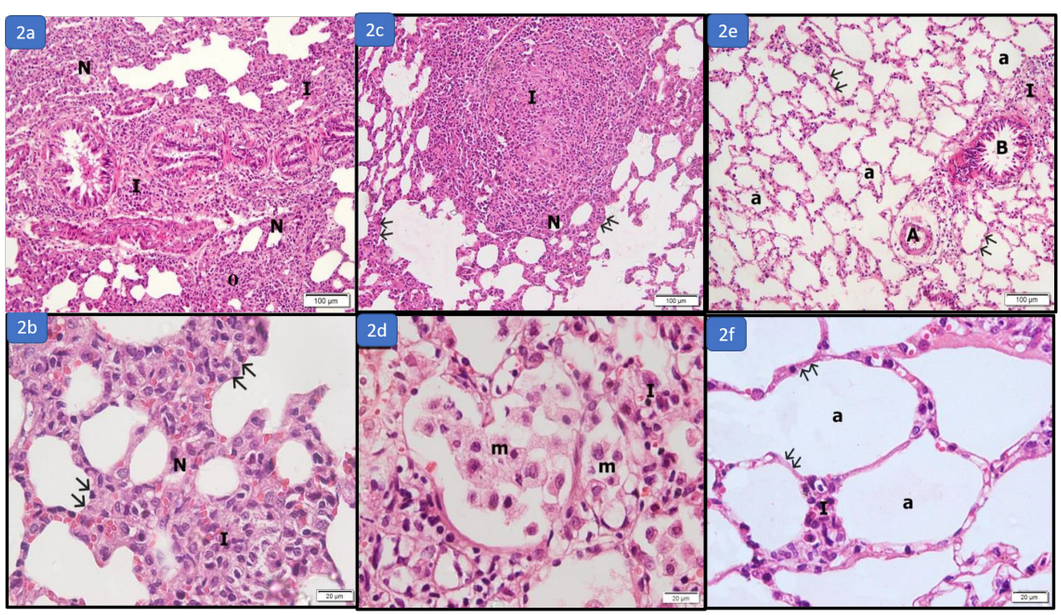

Fig. 2: Photomicrographs of sections in the lungs of rats stained with H&E (2a): group III, showing obvious narrowing (N) or even collapse (o) of alveolar spaces. Marked diffuse cellular infiltration (I) is also seen in the interstitium (x100). (2b): group III, showing markedly thickened interalveolar septa (arrows) with narrowing of the alveolar space (N). Obvious cellular infiltration (I) is also noticed. (x400). (2c):group IV, showing narrowing of alveolar spaces (N). Thickening of the alveolar walls and interalveolar septa (arrows) is noticed. Obvious cellular infiltration (I) is also seen in the interstitial tissue. (x100). (2d): group IV, Many alveoli contain numerous intra-alveolar macrophages (m) with abundant foamy pale acidophilic cytoplasm and medium sized round to oval nuclei. Mononuclear cellular infiltration (I) is also seen in the interstitium. (x400). (2e): group V,showing normal alveoli (a) with apparent interalveolar septa (arrows). Normal brochiole (B) and arteriole (A) are also seen. Mild cellular infiltration (I) is noticed in the interstitium. (x100). (2f): group V showing patent alveoli (a) with apparent thin alveolar walls (arrows) and mild cellular infiltration (I) in the interstitium. (x400).

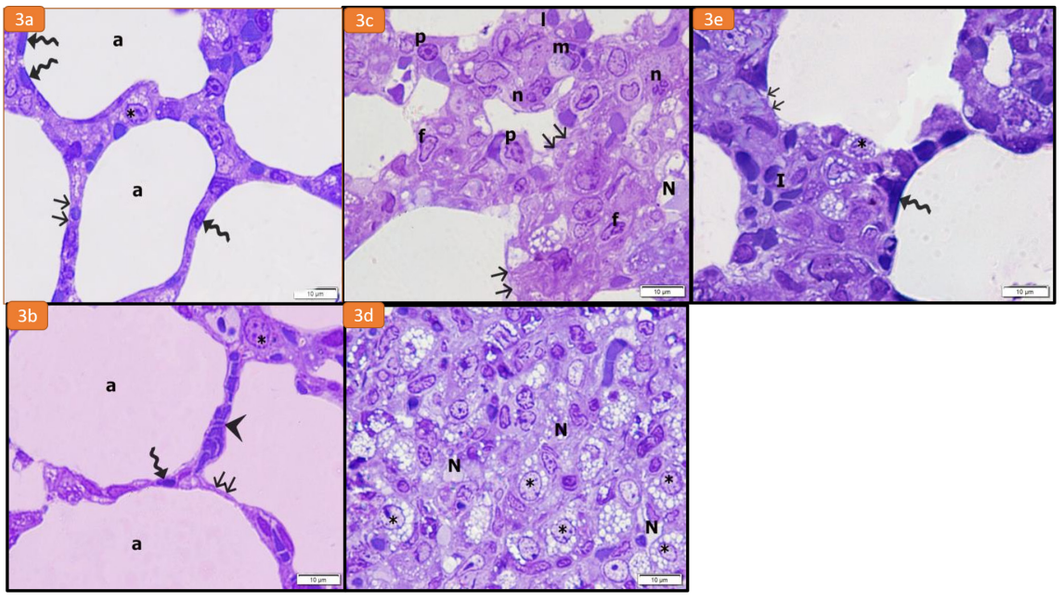

Fig. 3: Photomicrographs of sections in the lungs of rats stained with Toluidine blue (3a): control group showing alveoli (a) lined by type I flat cells exhibiting flat nuclei (wavy arrow) and type II which display round vesicular nuclei with prominent nucleolus and foamy cytoplasm (*) pneumocytes. The interalveolar septa (arrows) are thin containing pulmonary capillaries. (x1000).(3b):group II showing alveoli (a) lined by type I (wavy arrow) and type II (*) pneumocytes. Blood capillary (arrow head) in the thin interalveolar septum (arrows) is also noticed. (x1000). (3c):group III showing apparent thick interalveolar septa (arrows) with narrowing of alveolar space (N). Cellular infiltration containing neutrophils (n), small lymphocytes (l), plasma cells (p), macrophags (m) and fibroblasts (f) is seen in the interalveolar septa. (x1000).(3d):group IV showing prominent alveolar narrowing (N) as well as obvious appearance of type II pneumocytes (*) which appear as highly vacuolated cells.(x1000).(3e):group V showing normal alveolar lining with type I (wavy arrow) and type II (*) pneumocytes. Mild cellular infiltration (I) in apparently thick interalveolar septa is also noticed. (x1000).

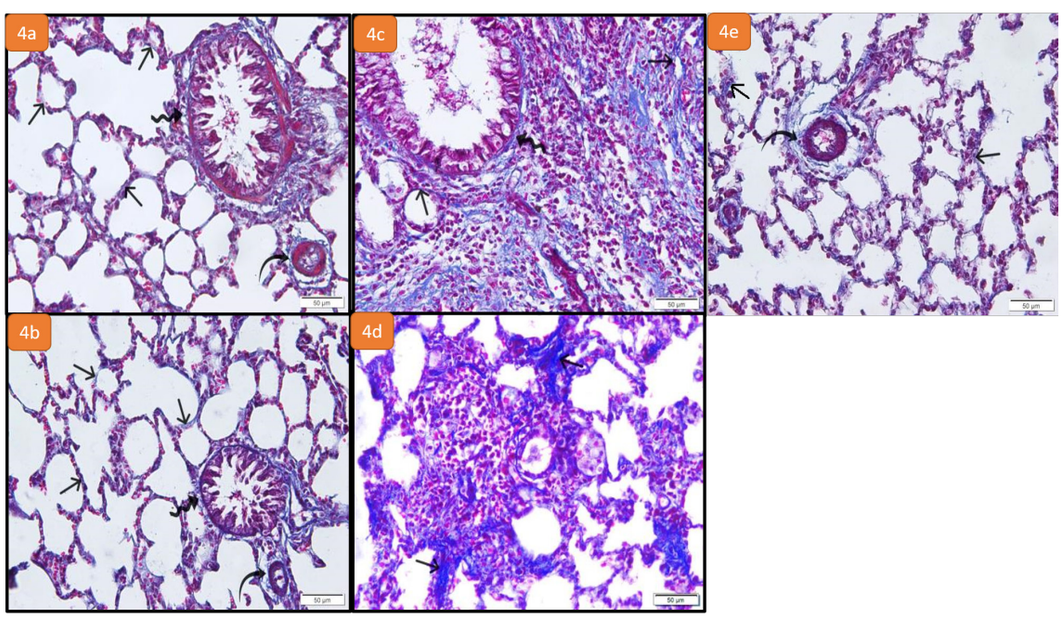

Fig. 4: Photomicrographs of sections in the lungs of rats stained with Masson's trichrome, (4a): control group showing fine collagen fibers in the interalveolar septa (arrow) and in the adventitia of the bronchiole (wavy arrow) and arteriole (curved arrows). (x200). (4b): group II showing fine collagen fibers in the interalveolar septa (arrows), in the adventitia of the bronchiole (wavy arrow) and that of an arteriole (curved arrow).(x200).(4c): group III, Deposition of collagen fibers in the wall of a bronchiole (wavy arrow). Collagen fibers in the thickened interalveolar septa (arrows) are also detected. (x200). (4d): group IV, showing deposition of collagen fibers in the interalveolar septa (arrows). (x200). (4e): group V, Fine collagen fibers in the interalveolar septa (arrows) and in the adventitia of an arteriole (curved arrow) are noticed. (x200).

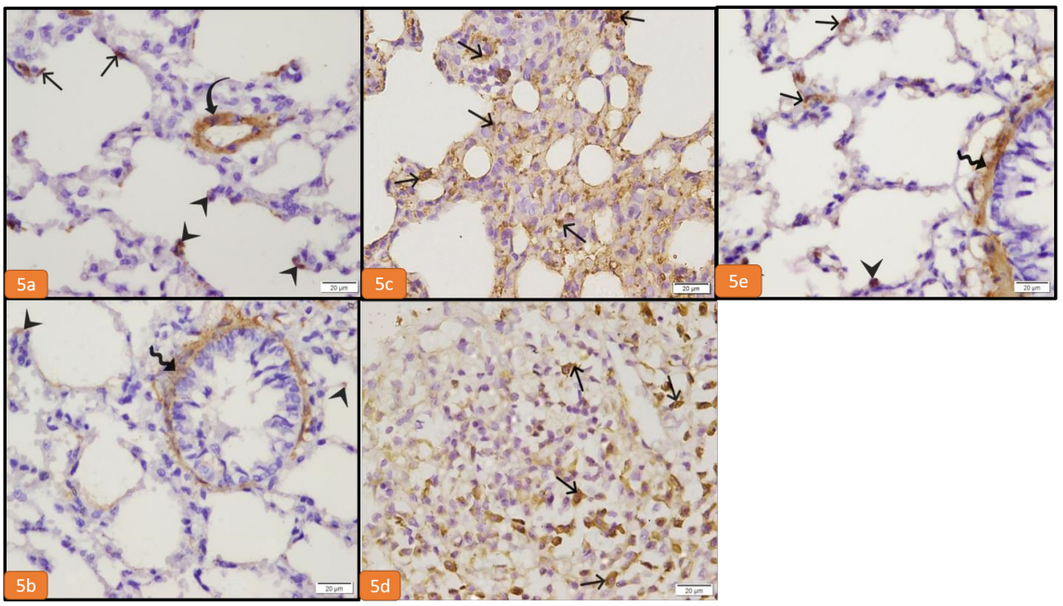

Fig. 5: Photomicrographs of sections in the lungs of rats stained with αSMA immunostaining(5a): control group, showing positive reaction in the knobs of the alveolar ducts (arrowheads) and in the tunica media of a blood vessel (curved arrow). Few immunopositive cells are seen in the alveolar wall (arrow). (x400). (5b): group II showing positive reaction in the knobs of the alveolar ducts(arrowheads). Positive reaction around bronchiole (wavy arrow) can be detected. (x400). (5c): group III, Many cells exhibit positive immunoreactivity for αSMA in the interalveolar septa (arrows). (x400). (5d): group IV, showing numerous cells with positive cytoplasmic immunoreaction in the interstitium and the interalveolar septa (arrows). (x400). (5e):group V, showing few cells with positive immunoreactivity for αSMA in the interalveolar septa (arrows). Positive reaction is also seen in the wall of bronchiole (wavy arrow) and also in knobs of alveolar ducts (arrowhead). (x400).

Table 1: Morphometric results

	Group I (control group)	Group II (pirfenidone group)	Group III (model group)	Group IV (recovery group)	Group V (treated group)
Mean area % of collagen (± SD)	3.3 ± 0.8	3.5 ± 0.6	10.9±1.6*	10.5±1.9*	5.6±1.1*#^
Mean area % of α SMA (± SD)	2.2 ± 0.4	1.8 ± 0.6	10.1±1.9*	10 ± 1.7*	4.7±1.1*#^

* Significant as compared to group I at $P<0.05$ # Significant as compared to group III at $P<0.05$ ^ Significant as compared to group IV at $P<0.05$

Table 2: Biochemical results

	Group I (control group)	Group II (pirfenidone group)	Group III (model group)	Group IV (recovery group)	Group V (treated group)
GSH level mmol/gm tissue	113.75 ± 1.9	107.4 ± 3.0	59.1 ± 4.7*	44.1 ± 6.3*	105.2± 4.4#^
MDA level nmol/gm tissue	32.1 ± 4.5	32.0 ± 9.3	85.3 ± 13.0*	106.8 ± 3.5*	48 ± 5.2#^

* Significant as compared to group I at $P<0.05$ # Significant as compared to group III at $P<0.05$ ^ Significant as compared to group IV at $P<0.05$

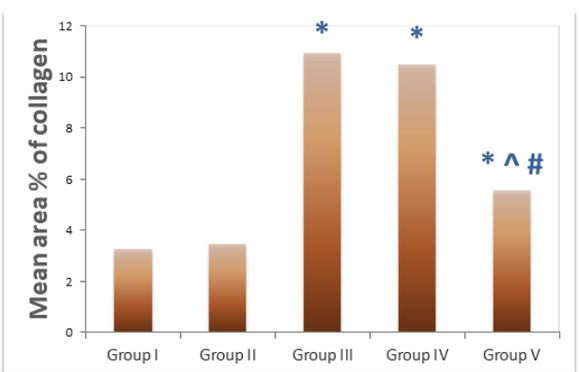

Histogram 1: Comparison between the mean area percent of collagen (± SD) in Masson's trichrome stained sections in all studied groups

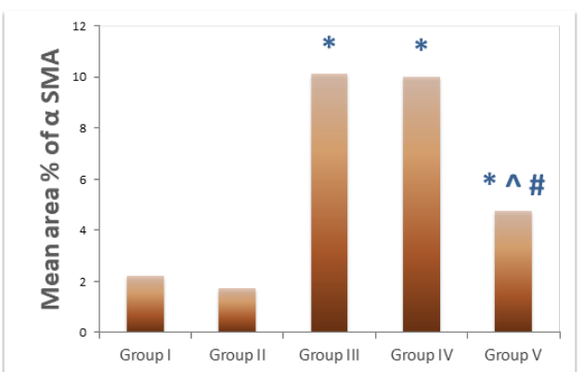

Histogram 2: Comparison between the mean area percent of α SMA (± SD) in immunostained sections in all studied groups

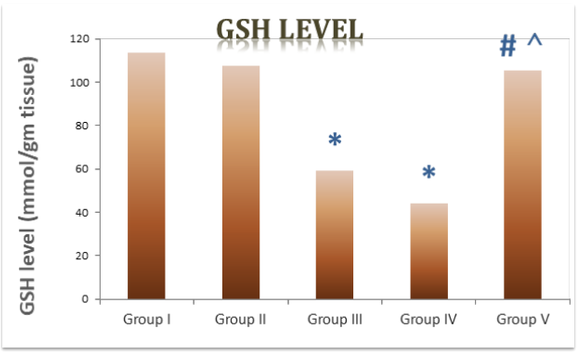

Histogram 3: Comparison between the mean values (± SD) of GSH levels in all studied groups

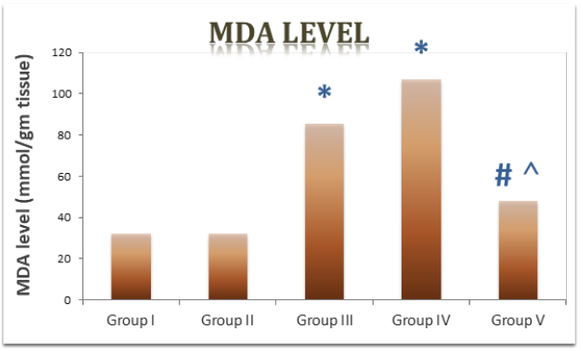

Histogram 4: Comparison between the mean values (± SD) of MDA levels in all studied groups

DISCUSSION

IPF is one of the most common and aggressive forms of lung fibrosis with high mortality and morbidity. It develops without an identified underlying cause and terminates with severe affection of lung functions. There are many risk factors for the development of IPF, the most important of which is cigarette smoking[22].

The present work aimed to develop an experimental model of IPF and to evaluate the therapeutic effect of pirfenidone, a newly introduced antifibrotic, on this model. Pirfenidone was chosen as it showed a promising potential effect as antifibrotic agent in various conditions such as acute kidney injury[10], choroidal neovascular fibrosis via a reduction in transforming growth factor (TGF-β2) mRNA levels and mature TGF-β2 protein levels[23] and cardiac diseases[24,25]. Reported that, pirfenidone leads to substantial regression of myocardial fibrosis in preclinical models.

IPF was induced in this study using bleomycin as it has been documented to be fast, effective and mimic the histopathology of human IPF to a great extend[26]. In previous studies, several routes of administration of bleomycin for induction of IPF were tried, however, intratracheal instillation of a single dose of 5 mg/kg has been reported to be the most effective[27,12]. So, bleomycin was administered as such in this study.

It was hypothesized that, bleomycin reaches the target cell where it binds to DNA and ferrous molecules. This complex has an oxidase-like activity that produces ROS. These free oxygen radicals cause lipid peroxidation, protein oxidation as well as breaks in the cellular DNA leading to cell damage. This mechanism is the basis of its use for the induction of lung fibrosis in animal models[28].

In the present study, the model group (group III) showed loss of normal lung architecture in the form of alveolar collapse, compensatory emphysematous changes and thickening of interalveolar septa. Similar findings were recorded[29]. The model group also showed marked interstitial and bronchiolar cellular infiltration. This infiltrate was formed of various inflammatory cells but was predominantly composed of neutrophils, lymphocytes, plasma cells and macrophages. These findings match[30], who performed bronchoalveolar lavage to mice with IPF model and found abundance of macrophages, lymphocytes and neutrophils in the collected fluid.

Suggested that acute lung injury starts to develop in the first week after local administration of bleomycin[5]. During this period, cell death of both type I and II pneumocytes followed by acute inflammation with recruitment of inflammatory cells commences. The release of pro-inflammatory cytokines and chemokines together with vascular leakage are the hallmark of this stage. This acute lung injury could explain the cause of deaths in our work, which could be due to sever anoxia of some rats. Added that bleomycin activity is amplified in lung and skin due to decreased levels of bleomycin hydrolase, an enzyme that deactivates bleomycin, in these tissues[31].

As demonstrated by Masson's trichrome stain, the model group in this study showed obvious collagen deposition around airways, blood vessels and also in the interalveolar septa. This was confirmed by the morphometric results as there was significant increase in mean area percentage of collagen in model group when compared to the control group. This was in accordance[32] who found a significant increase in hydroxyproline level, a marker of collagen content in tissue, in the model lung compared to the control.

It was recorded that, fibrosis starts to develop with a peak at the end of the second week after bleomycin administration. As the bleomycin induced chronic inflammation results in activation of fibroblasts into myofibroblasts which secrete extracellular matrix and deposit collagen[33].

Using α-SMA immunostaining, the lung of the model group revealed many positively stained cells that were evident in the interalveolar septa in comparison to the scarce presence of such cells in the control group. This was confirmed by the morphometric results where the area percentage of αSMA was significantly higher compared to the control group. Reported that α-SMA is

the functional marker of the fully matured myofibroblast it form contractile bodies together with myosin[34]. These bodies are responsible for the ability of myofibroblasts to migrate, contract and apply traction on ECM. The level of expression of αSMA is proportionate to the level of activity of myofibroblasts. moreover[35] have postulated that in oxidative stress, lung myofibroblasts resist apoptosis and continue to act irregularly resulting in a fibroporliferative state.

It was hypothesized that in IPF, chronic and repetitive alveolar epithelial cell injury occurs with subsequent release of various cytokines as TGFβ, platelet derived growth factor (PDGF), fibroblast growth factor (FGR) and vascular endothelial growth factor (VEGF)[36]. TGFβ was clarified to be the main contributor of disease progression[35]. It is secreted in an inactive form to the ECM where it is activated and stimulates transformation of fibroblasts into myofibroblasts which in turn secrete large amounts of collagen and ECM[37].

Though the main source of myofibroblasts is tissue fibroblasts but other sources have also been described. It could be originated from vascular smooth muscles, pericytes, mesenchymal stem cells, also from epithelialmesenchymal transitionin (EMT) of endothelial and epithelial cells, as type II pneumocytes. Differentiation into myofibroblasts occurs under certain conditions like mechanical tension, presence of certain ECM proteins and TGFβ. In addition to its role in the pathology of fibroproliferative disorders, myofibroblasts play a role in growth and metastasis of epithelial tumours[38].

In this study, the biochemical analysis of MDA and GSH clarified that the lungs of model group (group III) were in a state of oxidative stress. This was proved by morphometric results as there was significant increase in MDA and significant decrease in GSH concentration in group III when compared to the control group. These results concord[39] who measured multiple oxidative stress markers such as superoxide dismutase, catalase, glutathione peroxidase, GSH and MDA and found that all of them showed decreased tissue levels except MDA which showed increased levels.

GSH is one of the most potent and most abundant intracellular antioxidants. It is present mainly in the cytoplasm and to a lower extent in the mitochondria. It diffuses extracellularly and is detected in lung surfactant[40]. GSH is mostly present in the reduced form to act as a scavenger for ROS. Under normal conditions, balance is maintained but with chronic oxidative load, GSH is depleted resulting in high cellular ROS levels[41].

It was reported that oxidative stress affects cellular activity and aids in IPF progression. A two-way connection between oxidative stress and endoplasmic reticulum (ER) stress, a key factor in IPF, has been observed. This connection is also involved in the activation of inflammatory pathways which further increment the stress on the cells[42].

Furthermore, in IPF, abnormal activity of pro-oxidant enzymes has been detected in fibroblastic foci and alveolar epithelial cells. These enzymes increase ROS causing mitochondrial dysfunction, increased glycolysis and reduced GSH synthesis. Also, the produced ROS facilitate the action of TGFβ in initiating alveolar cell death, EMT and transformation of fibroblasts into myofibroblasts[43].

Intracellular ROS attack the cell membrane through polyunsaturated fatty acids disintegration, which clarifies MDA rise subsequent to bleomycin challenge. MDA is a reactive carbon agent that is used as a marker of lipid peroxidation. In line with the previous studies, the data showed that bleomycin endotracheal instillation induced a significant increase in the serum levels of MDA in bleomycin treated animals[44].

Lungs of the recovery group (group IV) revealed the same changes recorded in model group in addition to presence of many intra-alveolar foamy macrophages, these cells are a common nonspecific histopathological associate to inflammation and fibrosis in diseases involving obstruction of smaller airways[45]. These macrophages play an active role in IPF as they release inflammatory mediators as TNF-α, IL-1, IL-6 and IL-10. They also promote differentiation of stem cells into myofibroblasts and release of pro-fibrotic mediators as TGFβ. Last but not least, macrophages release free oxygen radicals that potentiate both inflammation and fibrosis in IPF[46].

The recovery group showed non-significant changes in all parameters measured reflecting that, there is no recovery without treatment. also it showed obvious appearance of type II pneumocytes which adopted highly vacuolated cytoplasm[47]. clarified that persistence of ER stress causes accumulation of misfolded proteins in the cellular cytoplasm which in turn causes cell death. It has been thought that ageing or certain genetic mutations make type II pneumocytes more susceptible to injury and cell hyperplasia that potentiate the development of IPF.

Many previous studies investigated a lot of drugs for their antifibrotic activity in treating IPF, but not many proved worthy. One of those is Nacetyl cysteine[48]. And simtuzumab[49].

Pirfenidone exhibits anti-inflammatory and antioxidant effects in addition to its antifibrotic activity. Rather than treatment of the cause, prifenidone is classified more as a disease-modifying drug that slows down the disease progression[50]. Studied the effect of pirfenidone on a pulmonary fibrosis rat model concluded that doses of 50 and 100mg/kg produced satisfactory results with a better effect than using the larger dose[13]. In accordance, a dose of 100mg/kg in the current study was used.

In this study, pirfenidone was administered 2 weeks after induction of IPF. Most studies started the administration of potential therapies during the first week following bleomycin delivery which coincide with the inflammatory phase of the model. This causes flawed results and

restriction of further usage of the agent as a treatment of IPF. It has been recommended to administer the potential therapy after passage of the inflammatory phase preferably after at least 10 days from bleomycin delivery[7].

The treated group (group V) revealed improvement of the lung architecture with a notable decrease in cellular infiltration and interalveolar wall thickening. There was a significant decrease in the mean area percentage of collagen in comparison to model and recovery groups. Also, there was a significant decrease in α-SMA positive cells when compared to both groups. Reported similar results as they found that pirfenidone reduced alveolar inflammation and damage[13]. They also added that it reduced deposition of collagen fibers. Additionally,[51] hypothesized that, pirfenidone causes inhibition of macrophage infiltration and subsequent inflammatory recruitment. Tested the therapeutic effect of pirfenidone on a pulmonary fibrosis model and found it effective in treating IPF[52].

Pirfenidone has an inhibitory effect on TGF-β level[48,53]. Through suppression of TGFβ-mediated pathways. It decreases transformation of fibroblast into myofibrobasts and their proliferation. It also inhibits expression of α-SMA in myofibroblasts[53]. Additionally, it inhibit tumor necrosis factor-alpha (TNFα), fibroblast growth factor (FGF) and reducing collagen type one. Pirfenidone also plays a role in the attenuation of fibroblasts[54].

Very recently,[55] suggested that pirfenidone as an anti-fibrotic drug with an anti-oxidant activity can prevent lung injury during SARS-CoV-2 infection. This done by blocking the maturation process of TGF-β and enhancing the protective role of peroxisome proliferator-activated receptors (PPARs). It may be an effective and safe choice for suppressing the inflammatory response during COVID-19. They recommended that, it would be a combination of pirfenidone and N-acetylcysteine to achieve maximum benefit during SARS-CoV-2 treatment.

Conforming to the histological results, the biochemical markers results of group V showed a decrease in the oxidative stress state with significant increase in GSH concentration and a significant decrease in MDA concentration when compared to model and recovery groups. These results match the findings of a recent clinical trial that evaluated the effect of pirfenidone on systemic oxidative stress and inflammation markers where a significant increase in antioxidant markers in plasma as GSH was reported[56].

CONCLUSION

1. Bleomycin model through IT instillation was a fast and overall a reliable model for induction of IPF in rat.
2. Pirfenidone could be considered a newly introduced drug for management of IPF as it protects against ROS, it decreased the number and activity of myofibroblasts and finally it had a potent antifibrotic activity.

RECOMMENDATIONS

- Bleomycin may be investigated to be used through oropharyngeal route.
- Further studies to know more about the pathogenesis of IPF and possible risk factors.
- Further studies and research of the exact target of pirfenidone and its effect on various cellular components.
- Investigation of other new antifibrotic drugs as ninetadinib and PBI-4050 and comparison of their effects with pirfenidone.
- Application of these drugs in clinical trials.
- Trying longer durations to evaluate the long term therapeutic effect of pirfenidone.

CONFLICT OF INTERESTS

There are no conflicts of interest.

REFERENCES

1. Kim S., Lim J.H., and Woo C.H.(2020). Therapeutic potential of targeting kinase inhibition in patients with idiopathic pulmonary fibrosis. Yeungnam Univ J Med, 37(4): 269–276.
2. Hadjicharalambous M. R., and Lindsay M. A. (2020). Idiopathic pulmonary fibrosis: Pathogenesis and the emerging role of long non-coding RNAs. International Journal of Molecular Sciences, 21(2): 1–19.
3. Tashiro J., Rubio G. A., Limper A. H., Williams K., Elliot S. J., Ninou I., Aidinis V., Tzouvelekis A., and Glassberg M. K. (2017). Exploring animal models that resemble idiopathic pulmonary fibrosis. Frontiers in Medicine, 4: 118–129.
4. Watson R. A., De La Peña H., Tsakok M. T., Joseph J., Stoneham S., Shamash J., Joffe J., Mazhar D., Traill Z., Ho L. P., Brand S., and Protheroe A. S. (2018). Development of a best-practice clinical guideline for the use of bleomycin in the treatment of germ cell tumours in the UK. British Journal of Cancer, 119(9): 1044–1051.
5. Liu T., De Los Santos F., and Phan S. (2017). The bleomycin model of pulmonary fibrosis. In: Methods in Molecular Biology, 1st ed., Humana Press, New York, 27–42.
6. Somogyi V., Chaudhuri N., Torrisi S. E., Kahn N., Müller V., and Kreuter M. (2019). The therapy of idiopathic pulmonary References 135 fibrosis: What is next? European Respiratory Review, 28(153): 1– 20.

7. Jenkins R. G., Moore B. B., Chambers R. C., Eickelberg O., Konigshoff M., Kolb M., Laurent G. J., Nanthakumar C. B., Olman M. A., Pardo A., Selman M., Sheppard D., Sime P. J., Tager A. M., Tatler A. L., Thannickal V. J., and White E. S. (2017). An official American thoracic society workshop report: Use of animal models for the preclinical assessment of potential therapies for pulmonary fibrosis. American Journal of Respiratory Cell and Molecular Biology, 56(5): 667–679.
8. Jiang N., Ma M., Li Y., Su T., Zhou X. Z., Ye L., Yuan Q., Zhu P., Min Y., Shi W., Xu X., Lv J., and Shao Y. (2018). The role of pirfenidone in alkali burn rat cornea. International Immunopharmacology, 64: 78–85.
9. Türkmen E., and Pata Y. S. (2019). Prevention of tracheal stenosis with pirfenidone after tracheotomy: An experimental study. Laryngoscope, 129(5): 178–189.
10. Lima-Posada I., Fontana F., Pérez-Villalva R., Berman-Parks N., and Bobadilla N. A. (2019). Pirfenidone prevents acute kidney injury in the rat. BMC Nephrology, 20(1): 158–167.
11. Peng L., Yang C., Yin J., Ge M., Wang S., Zhang G., Zhang Q., Xu F., Dai Z., Xie L., Li Y., Si J. Q., and Ma K. (2019). TGF-β2 induces Gli1 in a Smad3-dependent manner against cerebral ischemia/reperfusion injury after isoflurane post-conditioning in rats. Frontiers in Neuroscience, 13: 636–650.
12. Song X., Yu W., and Guo F. (2018). Pirfenidone suppresses bleomycin induced pulmonary fibrosis and periostin expression in rats. Experimental and Therapeutic Medicine, 16(3): 1800–1806.
13. Guo J., Yang Z., Jia Q., Bo C., Shao H., and Zhang Z. (2019). Pirfenidone inhibits epithelial-mesenchymal transition and pulmonary fibrosis in the rat silicosis model. Toxicology Letters, 300: 59–66.
14. Tian S., Cao W. F., Zhang Y. Y., and Wu Q. (2019). Effects of Yiqi Huayu Hutan decoction on pulmonary fibrosis in rats and its mechanism. Chinese journal of applied physiology, 35(2): 101–106.
15. Helms M. N., Torres-Gonzalez E., Goodson P., and Rojas M. (2010). Direct tracheal instillation of solutes into mouse lung. Journal of Visualized Experiments, (42): 2–4.
16. Aboul-Fotouh G. I., Zickri M. B., Metwally H. G., Ibrahim I. R., Kamar S. S., and Sakr W. (2015). Therapeutic effect of adipose derived stem cells versus atorvastatin on amiodarone induced lung injury in male rat. International Journal of Stem Cells, 8(2): 170–180.
17. Rahman I., Kode A., and Biswas S. K. (2007). Assay for quantitative determination of glutathione and glutathione disulfide levels using enzymatic recycling method. Nature Protocols, 1(6): 3159–3165.
18. Esterbauer H., and Cheeseman K. H. (1990). Determination of aldehydic lipid peroxidation products: Malonaldehyde and 4-hydroxynonenal. Methods in Enzymology, 186: 407–421.
19. Suvarna K. S., Layton C., and Bancroft J. D. (2018). The hematoxylins & eosin, connective tissue, mesenchymal tissue with their stains and Immunohistochemical techniques. In: Bancroft's Theory& Practice of Histological techniques, 7th ed., Elsevier, 173–214, 381–426.
20. Hunter E., Malony P., and Bendayan M. (1993). Fixation, Dehydration and Embedding, Cutting. In: Practical Electron Microscopy: A Beginner's Illustrated Guide, 2nd ed., Press Syndicate of the University of Cambridge, New York, 1–70.
21. Emsley R., Dunn G., and White I. R. (2010). Mediation and moderation of treatment effects in randomised controlled trials of complex interventions. Statistical Methods in Medical Research, 19(3): 237–270.
22. Zakaria D.M., Zahran N.M., Arafa S.A.A., Mehanna R.A. and Abdel-Moneim R.A. (2021). Histological and Physiological Studies of the Effect of Bone Marrow-Derived Mesenchymal Stem Cells on Bleomycin Induced Lung Fibrosis in Adult Albino Rats. Tissue Eng Regen Med, 18(1): 127–141.
23. Gao C., Cao X., Huang L., Bao Y., Li T., Di Y., Wu L. and Song Y. (2021). Pirfenidone Alleviates Choroidal Neovascular Fibrosis through TGF- β/Smad Signaling Pathway. J Ophthalmol 2021 Feb 10;2021:8846708.
24. Aimo A., Cerbai E., Bartolucci G., Adamo L., Barison A., Lo Surdo G., Biagini S., Passino C., and Emdin M. (2020). Pirfenidone is a cardioprotective drug: Mechanisms of action and preclinical evidence. Pharmacological Research, 155: 104694.
25. Lewis G.A., Schelbert E.B., Naish J.H., Bedson E., Dodd S., Eccleson H., Clayton D., Jimenez B.D., McDonagh T., Williams S.G., Cooper A., Cunnington C., Ahmed F.Z., Viswesvaraiah R., Russell S., Neubauer S., Williamson P.R. and Miller C.A. (2019). Pirfenidone in Heart Failure with Preserved Ejection Fraction—Rationale and Design of the PIROUETTE Trial. Cardiovasc Drugs Ther, 33(4): 461–470.
26. Barbayianni I., Ninou I., Tzouvelekis A., and Aidinis V. (2018). Bleomycin revisited: A direct comparison of the intratracheal micro-spraying and the oropharyngeal aspiration routes of bleomycin administration in mice. Frontiers in Medicine, 5: 269–275.

27. Moore B. B., Lawson W. E., Oury T. D., Sisson T. H., Raghavendran K., and Hogaboam C. M. (2013). Animal Models of Fibrotic Lung Disease. American Jouranl of Respiratory Cell and Molecular Biology, 49(2): 167–179.

28. Arkema J. R. ., Nikula K. J., and Haschek W. M. (2013). Respiratory System. In: Haschek and Rousseaux's Handbook of Toxicologic Pathology, 3rd ed., Academic Press, London, 1935–2003.

29. Hemmati A. A., Jalali A., and Keshavarz P. (2018). Effect of chamomile hydroalcoholic extract on bleomycin-induced pulmonary fibrosis in rat. Tanaffos, 17(4): 264–271.

30. Tanaka K. I., Niino T., Ishihara T., Takafuji A., Takayama T., Kanda Y., Sugizaki T., Tamura F., Kurotsu S., Kawahara M., and Mizushima T. (2017). Protective and therapeutic effect of felodipine against bleomycin-induced pulmonary fibrosis in mice. Scientific Reports, 7(1): 1–12.

31. Serrano J., Avigan M., Koh C., and Sherker A. H. (2017). Bleomycin. In: LiverTox: Clinical and Research Information on Drug-Induced Liver Injury [online book], Retrieved from "https:// www.ncbi.nlm.nih.gov/books/NBK548499/."

32. Li L., Li Q., Wei L., Wang Z., Ma W., Liu F., Shen Y., Zhang S., Zhang X., Li H., and Qian Y. (2019). Dexamethasone combined with berberine is an effective therapy for bleomycin induced pulmonary fibrosis in rats. Experimental and Therapeutic Medicine, 18: 2385–2392.

33. Schiller H. B., Fernandez I. E., Burgstaller G., Schaab C., Scheltema R. A., Schwarzmayr T., Strom T. M., Eickelberg O., and Mann M. (2015). Time- and compartment-resolved proteome profiling of the extracellular niche in lung injury and repair. Molecular Systems Biology, 11(7): 819.

34. Stempien-Otero A., Kim D.-H., and Davis J. (2016). Molecular networks underlying myofibroblast fate and fibrosis. J Mol Cell Cardiol., 97: 153–161.

35. Penke L., and Peters-Golden M. (2019). Molecular determinants of mesenchymal cell activation in fibroproliferative diseases. Cellular and Molecular Life Sciences, 76(21): 4179–4201.

36. Knudsen L., Ruppert C., and Ochs M. (2017). Tissue remodelling in pulmonary fibrosis. Cell and Tissue Research, 367(3): 607–626.

37. Betensley A., Sharif R., and Karamichos D. (2016). A Systematic Review of the Role of Dysfunctional Wound Healing in the Pathogenesis and Treatment of Idiopathic Pulmonary Fibrosis. Journal of Clinical Medicine, 6(1): 2–21.

38. Carthy J. M. (2017). TGFβ signaling and the control of myofibroblast differentiation: Implications for chronic inflammatory disorders. Journal of Cellular Physiology, 233(1): 98–106.

39. Shariati S., Kalantar H., Pashmforosh M., Mansouri E., and Khodayar M. J. (2019). Epicatechin protective effects on bleomycin-induced pulmonary oxidative stress and fibrosis in mice. Biomedicine and Pharmacotherapy, 114: 1–10.

40. Vliet A. van der, Janssen-Heininger Y. M. W., and Anathy V. (2018). Oxidative stress in chronic lung disease: from mitochondrial dysfunction to dysregulated redox signalling. Molecular Aspects of Medicine, 63: 59–69.

41. Lv H., Zhen C., Liu J., Yang P., Hu L., and Shang P. (2019). Unraveling the potential role of glutathione in multiple forms of cell death in cancer therapy. Oxidative Medicine and Cellular Longevity, 2019: 1–16.

42. Chen A. C. H., Burr L., and McGuckin M. A. (2018). Oxidative and endoplasmic reticulum stress in respiratory disease. Clinical and Translational Immunology, 7(6): 1–13.

43. Cameli P., Carleo A., Bergantini L., Landi C., Prasse A., and Bargagli E. (2020). Oxidant/Antioxidant Disequilibrium in Idiopathic Pulmonary Fibrosis Pathogenesis. Inflammation, 43(1): 1–7.

44. Ramezani S., Javadi I., Kokhdan E.P., Omidifar N., Nikbakht J., Sadeghi H., Doustimotlagh A.H., Danaei N., Abbasi R. and Sadeghi H. (2021). Protective and therapeutic effects of ethanolic extract of Nasturtium officinale (watercress) and vitamin E against bleomycin-induced pulmonary fibrosis in rats. Res Pharm Sci, 16(1): 94–102.

45. Rossi G., Cavazza A., Spagnolo P., Bellafiore S., Kuhn E., Carassai P., Caramanico L., Montanari G., Cappiello G., Andreani A., Bono F., and Nannini N. (2017). The role of macrophages in interstitial lung diseases. European Respiratory Review, 26(145): 1–16.

46. Hamam G. G., Raafat M. H., and Kk Mostafa H. (2019). Histological study on possible therapeutic effect of BM-MSCs on healing of lung fibrosis induced by CCl 4 with reference to macrophage plasticity. Journal of Cytology & Histology, 10(2): 1–9.

47. Kropski J. A., and Blackwell T. S. (2019). Progress in understanding and treating idiopathic pulmonary fibrosis. Annu Rev Med., 70(3): 211–224.

48. Myllärniemi M., and Kaarteenaho R. (2015). Pharmacological treatment of idiopathic pulmonary fibrosis – preclinical and clinical studies of pirfenidone, nintedanib, and N-acetylcysteine. European Clinical Respiratory Journal, 2(1): 1–11.

49. Simtuzumab. (2019). Simtuzumab At a glance. Adis Insight-Springer, Retrieved from "https://adisinsight. springer.com/drugs /800032453."

50. Collins B. F., and Raghu G. (2019). Antifibrotic therapy for fibrotic lung disease beyond idiopathic pulmonary fibrosis. European Respiratory Review, 28(153): 1–15.

51. Chen J. F., Ni H. F., Pan M. M., Liu H., Xu M., Zhang M. H., and Liu B. C. (2013). Pirfenidone inhibits macrophage infiltration in 5/6 nephrectomized rats. American Journal of Physiology, 304(6): 676–685.

52. Rasooli R., Pourgholamhosein F., Kamali Y., Nabipour F., and Mandegary A. (2018). Combination therapy with pirfenidone plus prednisolone ameliorates paraquat-induced pulmonary fibrosis. Inflammation, 41(1): 134–142.

53. Bellaye P.-S., Yanagihara T., Granton E., Sato S., Shimbori C., Upagupta C., Imani J., Hambly N., Ask K., Gauldie J., Iglarz M., and Kolb M. (2018). Macitentan reduces progression of TGF-α1-induced pulmonary fibrosis and pulmonary hypertension. European Respiratory Journal, 52(2): 1–15.

54. Shah PV, Balani P, Lopez AR, Nobleza CMN, Siddiqui M, Khan S (2021): A Review of Pirfenidone as an Anti-Fibrotic in Idiopathic Pulmonary Fibrosis and Its Probable Role in Other Diseases. Cureus. 2021 Jan; 13(1): e12482.

55. Hamidi S.H., Veethil S.K., Hamidi S.H. (2021). Role of pirfenidone in TGF-β pathways and other inflammatory pathways in acute respiratory syndrome coronavirus 2 (SARS-Cov-2) infection: a theoretical perspective Pharmacol Rep, 73(3):712-727.

56. Fois A. G., Sotgiu E., Scano V., Negri S., Mellino S., Zinellu E., Pirina P., Pintus G., Carru C., Mangoni A. A., and Zinellu A. (2020). Effects of pirfenidone and nintedanib on markers of systemic oxidative stress and inflammation in patients with idiopathic pulmonary fibrosis: A preliminary report. Antioxidants, 9(11): 1–15.

الملخص العربى

تقييم هستولوجي ومناعي وبيوكيميائي للتأثير العلاجى المحتمل للبيرفيندون علي تليف الرئة المستحث بالبليوميسين في ذكور الجرذان البيضاء البالغة

هند شفيق بسيوني، نجلاء محمد سلامه، الاء سراج الدين حبيب، اسماء محمد عبدالحميد

قسم الهستولوجيا، كليه الطب، جامعه القاهره

خلفية العمل وهدفه: التليف الرئوي مجهول السبب هو مرض غير معروف سببه ويؤدي الي تليف في نسيج الرئة مع طبيعة تقدمية لا رجعة فيها وعدم وجود علاج مناسب ، لذلك اجريت هذه الدراسة لتقييم التأثير العلاجي للبيرفينيدون على التليف الرئوي المستحث بالبليوميسين في الجرذان.

المواد والطرق: تم استخدم ثلاثون من ذكور الجرذان البيضاء في هذه الدراسه. قسمت الي ٥ مجموعات: المجموعة الأولى (المجموعة الضابطة) ، المجموعة الثانية (مجموعة بريفينيدون) ، المجموعة الثالثة (مجموعة النموذج) ، المجموعة الرابعة (مجموعة التعافي) والمجموعة الخامسة (المجموعة المعالجة). تم أخذ عينات الرئة من جرذان المجموعة الاولي أ والمجموعة الثالثة في اليوم الرابع عشر من التجربه بينما تم أخذ عينات من باقي المجموعات في اليوم الثامن والعشرين من التجربة. تم إخضاع العينات لتحليل كيميائي حيوي لمالونديالديهيد والجلوتاثيون بالإضافة إلى دراسة نسيجية باستخدام صبغه الهيماتوكسيلين والايوسين،صبغه ماسون ثلاثي الألوان ، صبغة توليدين الزرقاء للشرائح الرقيقه وصبغة كيميائية مناعية لبروتين العضلات الملساء الفا. تم قياس متوسط النسبة المئوية لمساحة الكولاجين والخلايا الايجابيه لبروتين العضلات الملساء الفا وتحليلها إحصائيًا باستخدام محلل الصور.

النتائج: أظهرت المجموعتان الثالثة والرابعة ترسب الكولاجين في الحاجز السميك بين الحويصلات وتسلل الخلايا المسببه للالتهاب للأنسجة البين خلويه مما تسبب في ضيق أو حتى انغلاق كامل للحويصلات الهوائية. كانت هناك زيادة ذو دلاله احصائيه في متوسط النسبة المئوية لمساحة الكولاجين والخلايا الايجابيه لبروتين العضلات الملساء الفا مع انخفاض كبير في الجلوتاثيون وزيادة ملحوظة في المالونديالديهيد مقارنةً بالمجموعه الضابطه. وفي الوقت نفسه ، أظهرت المجموعة الخامسة استعادة بنية الرئة الطبيعية. كان هناك انخفاض كبيرفي متوسط النسبة المئوية لمساحة الكولاجين والخلايا الايجابيه لبروتين العضلات الملساء الفا، وانخفاض كبير في الجلوتاثيون وزيادة ملحوظة في المالونديالديهيد مقارنة بالمجموعتين الثالثة والرابعة.

الخلاصة: البيرفينيدون كان فعالاً كعامل مضاد للتليف مع انخفاض كبير في التليف والإجهاد التأكسدي في نموذج الجرذان لتليف الرئة.